PAPER

Check for updates

Pinewood and wheat straw bio-oil aqueous phase electrochemical hydrogenation utilising a PtRu/ACC catalyst

Cesar Catizane, [iD] *[a] Ying Jiang,[b] Scott Banks[c] and Joy Sumner*[d]

Bio-oil from biomass pyrolysis contains a wide range of oxygenated compounds, limiting its direct use as a fuel due to chemical instability and low energy density. This study investigates the application of electrochemical hydrogenation (ECH) as an alternative to the conventional hydrogenation process to upgrade bio-oil derived from wheat straw and pinewood. Experiments were conducted in a two-chamber electrochemical cell, with ECH conditions optimised based on prior research. Platinum–ruthenium on activated carbon cloth (PtRu/ACC) was selected as the catalyst for ECH reactions. The process preferentially reduced phenolic and carbonyl compounds while increasing the concentration of alcohols, as confirmed by gas chromatography-mass spectrometry (GC-MS) and Fourier transform infrared spectroscopy (FTIR) analyses. The ECH study revealed substantial reductions in phenolic compounds, notably p-cresol (62.1%) and phenol (29.3%), alongside an increase in alcohol content from 49.3% to 56.5% in pinewood-derived bio-oil. These chemical transformations demonstrate ECH's potential as a milder, more sustainable alternative to traditional hydrodeoxygenation processes. This study provides insights into the ECH process and suggests future directions for optimising bio-oil upgrading and supporting the development of renewable fuels.

1. Introduction

The global transition to sustainable energy sources necessitates reducing dependence on fossil fuels and mitigating greenhouse gas emissions. As concerns about climate change and resource depletion grow, biomass has been recognised as an important renewable resource for the production of fuels and chemicals. One particularly attractive product from biomass is bio-oil, generated through the pyrolysis of organic materials, including agricultural residues or woody biomass.[1] Bio-oil is a complex liquid comprising a wide range of organic compounds, including acids, alcohols, phenols, and ketones.[2–6] However, several characteristics of bio-oil, such as its chemical instability, high acidity, and low energy density, limit its direct use as a fuel.[7,8]

To realise the potential of biomass-derived bio-oil as a viable energy source, upgrading processes are necessary to reduce its oxygen content, thereby enhancing its chemical stability and

calorific value.[9] Conventional hydrogenation techniques, including hydrodeoxygenation (HDO), require high pressures and elevated temperatures, typically around 300 bar and 700 °C. Additionally, the conventional process requires using an external source of hydrogen gas, therefore further increasing the energy intensity and the costs of operation.[10–15] As an alternative, electrochemical hydrogenation (ECH) has emerged as a promising approach. ECH operates under milder reaction conditions, using electricity to generate hydrogen *in situ*, which then reacts with bio-oil constituents to reduce their oxygen content. This method offers the potential for improved energy efficiency and selectivity, enabling targeted modification of specific functional groups in bio-oil, such as phenolic compounds and carbonyl groups, constituting a significant proportion of its composition.[7–9,11,12,14–23]

Despite its advantages, the practical implementation of ECH for bio-oil upgrading remains challenging. Key aspects, such as understanding the behaviour of various organic compounds under electrochemical conditions and optimising catalyst performance, must be addressed to improve process efficiency. Additionally, the high chemical diversity of bio-oil complicates the upgrading process, as each compound class may exhibit different reactivity and require tailored catalytic conditions. Furthermore, the combination of different compounds in the mixture can lead to side reactions, synergistic and anti-synergistic effects during ECH.[24,25] Crucially, while ECH has shown promise with model compounds, there remains

[a]*School of Water, Energy and Environment, Cranfield University, Cranfield, MK43 0AL, UK. E-mail: cesar.catizane@cranfield.ac.uk*

[b]*Renewable and Sustainable Energy Research Centre, Technology Innovation Institute, Abu Dhabi, United Arab Emirates*

[c]*College of Engineering and Physical Sciences, Aston University, Birmingham, B4 7ET, UK*

[d]*Franco-Australian Centre for Energy, Swinburne University of Technology, Melbourne, Australia*

a significant knowledge gap in its direct application and understanding for complex, real bio-oil mixtures, which are far more representative of actual industrial feedstocks.

Pyrolysis bio-oils can be divided into two distinct phases: the more viscous, apolar, non-aqueous "oily" phase and the water-soluble "aqueous" phase. While the aqueous phase is soluble in conventional water-based electrolytes, the oily phase is hydrophobic and poorly compatible with these systems, severely limiting the efficiency of traditional ECH processes. This study specifically addresses this critical gap by investigating the ECH of bio-oil derived from the slow pyrolysis of wheat straw and pinewood, focusing on the aqueous fractions. This focus is necessitated by the unique challenges and opportunities presented by the aqueous phase, which is rich in highly oxygenated compounds but often overlooked in direct ECH studies despite its substantial volume and distinct chemical profile.

For this application, the selected catalytic cathode needs to be versatile enough to convert a variety of compounds, unlike those designed specifically for model compound experiments. Both ruthenium and platinum have demonstrated success in facilitating the ECH process. Du $et\ al.$ reported that Pt_3Ru/ACC achieves a higher conversion rate than either Pt or Ru alone, likely due to a synergistic effect between the two metals, where platinum excels in hydrogenation and ruthenium predominantly enhances direct hydrogenolysis, the cleavage of chemical bonds by reaction with hydrogen.[26] Additionally, Salakhum $et\ al.$ found that combining these metals lowers the heterolytic activation energies for cleaving C–O and O–H bonds.[27] Based on these findings, this work employs a platinum–ruthenium on activated carbon cloth (PtRu/ACC) catalyst to hydrogenate bio-oil components, aiming to improve their stability, energy density and corrosivity. The research seeks to elucidate the impact of the ECH process on various chemical groups and assess its effectiveness in transforming bio-oil into a more stable and energy-dense product.

Through its direct application of ECH to challenging, real bio-oil aqueous phases, this study offers novel and valuable insights into the selectivity, efficiency, and mechanistic complexities of the procedure that cannot be fully captured by model compound studies. By advancing our understanding of ECH and its application to such intricate systems, this research takes a crucial and innovative step towards developing practical and scalable solutions for renewable fuel production, directly addressing the urgent global need for cleaner, sustainable energy alternatives.

2. Materials and methodologies

2.1. Materials

Sulphuric acid solution (5 M) and toluene (99.5%) were purchased from Thermo Fisher Scientific. All chemicals were used as received without further purification. A Nafion 117 membrane (Ion Power Inc. PA, USA) was used as the cation exchange membrane to separate the cathode and anode chambers. To ensure the activation of the membrane and optimise its ion transport capability, it was pretreated according

to the methodology of Peng $et\ al.$[28] treatment in oxygen peroxide (H_2O_2) at 80 °C, followed by deionised water and 1.0 M H_2SO_4 at the same temperature. Each step in the pretreatment of the membrane duration was 1 h, and the membrane was washed with DI water after each step.

2.2. Biomass pyrolysis

Slow pyrolysis experiments were conducted to generate bio-oil using a screw auger reactor with a processing capacity of 100 to 200 kg h^{-1} (subject to feedstock density). The system consists of four main sections: the feeding system, the slow pyrolysis reactor, the vapour condensation liquids collection system, and the char cooling and product outlet. The feeding system includes a metered screw-feed unit supplying a nitrogen-purged interlocked twin-valve airlock arrangement. A single-pass setup was employed to allow the collection and analysis of the gas stream (comprising nitrogen and non-condensable product gas). The experiments targeted an average pyrolysis temperature of 500 ± 5 °C for pinewood and 550 ± 5 °C for wheat straw, with a solid's residence time in the reactor of 20 minutes. These temperatures were chosen to optimise the yield and composition of the bio-oil for each specific feedstock, accounting for their varying lignocellulosic compositions and thermal behaviour. The pyrolysis vapours and non-condensable gases exit the pyrolysis chamber at a high level via trace-heated pipework to the condensation system, with char exiting via a cooling screw and a second nitrogen-purged and interlocked twin-valve airlock on the outlet.

The vapours were condensed in a recirculated and temperature-controlled spray quench column, using ISOPAR™ (Isopar V, CAS number: 64742-46-7) as the initial quenching medium, which becomes increasingly diluted with the condensed products that accumulate in the liquid's sump. Spray condensation liquids are temperature controlled (25 and 30 °C) via a separate water-cooling circuit and heat exchanger arrangement. Aerosols are coalesced in a wet-walled electrostatic precipitator operating at 12.5 kV and 0.5 mA, flushed with a combination of ISOPAR™ and condensed pyrolysis liquids. The pyrolysis liquid is gravity separated from the ISOPAR™ at the end of each experiment in the collection tank. The pyrolysis liquid separates into two distinct phases: an organic phase and an aqueous phase. These are divided by gravity using a separation funnel. After passing through the electrostatic precipitator, the remaining gases are routed via a gas flowmeter to a flare.

2.3. Electrochemical hydrogenation

A two-chamber electrochemical cell, separated by a cation exchange membrane (CEM), was selected for the ECH process (see Fig. 1). The utilised cathode is a 2 × 2 cm, 4 mg cm^{-2} platinum ruthenium black-carbon cloth electrode (PtRu/ACC, Fuel Cell Store Inc., Texas, USA, 1 : 1 Pt : Ru ratio), and the counter electrode was a platinum plate (1 × 1 cm, Ossila). The full characterisation of the cathode was conducted in a previous study.[24] This previous work included detailed analysis of the catalyst's electrochemical performance, such as its faradaic efficiency for hydrogen evolution and hydrogenation reactions.
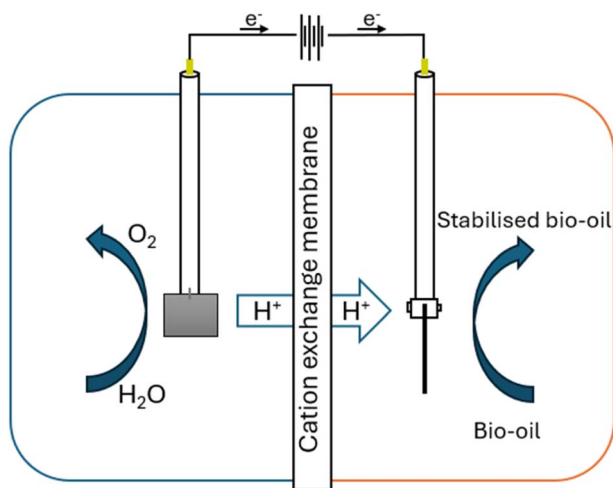
Fig. 1 H-Type electrochemical cell utilised for ECH. The cell consists of the anode chamber, where the water oxidation happens, a cation exchange membrane and the cathode chamber, where the hydrogenation process happens.

The electrodes were held at a 14 cm distance from each other. The membrane had a circular area with a diameter of 1 cm. An Ag/AgCl (in saturated KCl solution) as the reference electrode.

The PtRu/ACC cathode was selected for its proven efficacy in facilitating hydrogenation reactions, while the constant temperature and current density were optimised based on prior studies. For all experiments, both the anode and cathode chambers were filled with 90 mL of 1 M sulfuric acid.

Each test was initiated under electrostatic control (25.0 mA cm^{-2}) and constant temperature (55 °C) for 10 minutes without the organic compounds to polarise the electrodes. The aqueous phase of the bio-oil was filtered to remove any solid contaminants and reduce membrane and cathode fouling. After that, 1 mL of the prepared bio-oil was added to the system. The experiment was run for 5 h to ensure the availability of enough electrons in the system to convert the compounds. Samples (1 mL) were taken, and the organic compounds were extracted with 2 mL of dichloromethane (DCM). A toluene solution (0.2 mL) was added to each vial as an internal standard. After each experiment, the electrolyte was discarded, the cell cleaned, and the cathode was soaked in 5 mL DCM for 15 min to ensure the desorption of any molecules on its surface.

As the bio-oil is not stable, several side reactions could take place during the experiment, especially due to the addition of heat into the system. Therefore, a control experiment was conducted by maintaining the system under identical conditions without applying current to distinguish between electrochemical and non-electrochemical effects. All tests were carried out in triplicate.

2.4. Analytical methods

The samples were taken for analysis in the GC-MS Shimadzu TQ8040. The GC used a Restek Rtx-5 capillary column, 28.5 m × 0.25 mm with a 0.25 μm film thickness, a 1.18 mL per min helium carrier gas flow rate, and a split ratio of 1 : 25. The

injector temperature was set at 250 °C. The GC oven program started at 34 °C and was held for 2 min. Then, it was heated at 50 °C min^{-1} to 300 °C. Mass spectrometry was operated with m/z ranging from 50 to 500. Species associated with each chromatographic peak were identified by comparing their observed mass spectrum with the NIST library and then confirmed by injection of authentic samples. External standards were also used to identify compounds and quantify the peaks. Results are in area%. Reduction in concentration was calculated according to:

$$R_c = 1 - \frac{F_c}{I_c} \times 100 \tag{1}$$

where R_c is the reduction in concentration, F_c is the initial concentration, and I_c is the final concentration. When the initial is higher than the final concentration, a "−" sign will be used to refer to R_c. When the initial concentration is 0 R_c will be classified as "−100.00%. The reduction in relative area (R_a) is:

$$R_a = F_c - I_c \tag{2}$$

Fourier transform infrared spectroscopy was carried out in a Shimadzu IRTracer-100 and scanned in transmittance mode. The scans were made 10 times from 500 to 4000 cm^{-1} with a resolution of 4 cm^{-1} with Happ-Genzel apodization.

3. Results

3.1. ECH of the aqueous phase

The electrochemical hydrogenation of the aqueous phase derived from the slow pyrolysis of wheat straw and pinewood (herein referred to as WS_{aq} and PW_{aq}, respectively) was performed at the optimal conditions established in our previous study[24] (temperature = 55 °C, current density = 25.0 mA cm^{-2}). The primary goal was to reduce the oxygenated and nitrogenous compounds, enhancing the hydrogen content of the bio-oil (C : H ratio), improving stability, corrosivity and heating values. Fig. 2 presents some of the primary components of both WS_{aq} and PW_{aq} before and after ECH, showcasing the chemical transformations during the process.

The hydrogenation of organic compounds over PtRu/ACC follows the Langmuir–Hinshelwood mechanism[29,30] (Fig. 3), where both reactants adsorb onto the catalyst surface before they react with each other, and the catalyst provides a surface that lowers the activation energy needed for the reaction. Once the reaction occurs, the product molecules desorb from the catalyst surface and are released into the liquid phase. Therefore, more than one molecule in the system can lead to competition for the active adsorption sites, lowering activity and hindering the hydrogenation process. If the two species ("A" and "B") are hydrogen atoms, they could form hydrogen gas (H_2), a process known as hydrogen evolution reaction (HER), which is the competing reaction for ECH and can form bubbles that impede the adsorption process.

Bio-oils are complex mixtures containing up to hundreds of compounds. Therefore, only the largest significant peaks were identifiable and quantifiable via GC-MS. Table 1 shows the
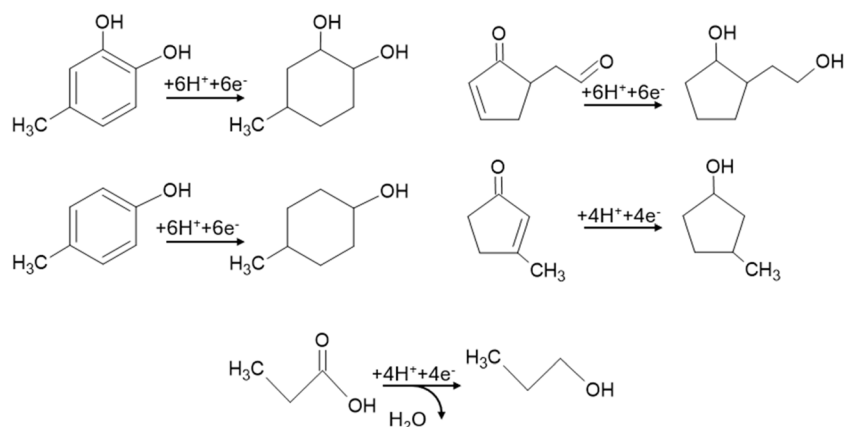
Fig. 2 Some of the main compounds found in the aqueous phase of bio-oils and their respective products after hydrogenation.

main peaks before and after the ECH of PW_{aq}. Toluene was used as an internal standard, so its concentration is set to 1.00. It is important to understand that the hydrogenation of compounds containing rings typically starts with the saturation of the ring, followed by the hydrogenation of any side chains. Therefore, a decrease in the concentration of phenol derivatives does not necessarily indicate a reduction in the relative concentration of alcohols. For instance, while the concentration of phenol decreased by 29.27%, cyclohexanol, a fully saturated ring compound with an alcohol group, was found among the products resulting from phenol's hydrogenation. Signifying a reduction in phenol concentration, whereas the alcohol concentration was unaltered.

Notable results include the conversion rates of *p*-cresol and 2-methyl phenol, at 62.10 and 55.73%, respectively, and the complete depletion of 4-methyl-1,2-benzenediol and 3-methyl-1,2-benzenediol. In addition, propanoic acid presented the second-lowest conversion, at 8.23%, where the lower value was expected, as carboxylic acids are resistant to ECH due to the low

electrophilicity of carbonyl carbon atom and the relative stability of the C=O bond.[31–33] For both feedstocks, on average, alcohols presented the highest tendency for reduction, followed by other oxygenated compounds, such as ketones and ethers, and carboxylic acids presented the lowest conversion rate.

Table 2 shows the change in concentration of the most common compounds in WS_{aq} before and after ECH. The compounds that underwent the largest change in concentration were mostly the same as in PW_{aq}, although full depletion was not achieved. As most of the compounds are aromatics, this explains the reduction in the number of unsaturated rings found during FTIR (Fig. 4c and d). Other notable results include cyclopentanone, 3,5-dimethyl-phenol and 2-oxo-3-cyclopentene-1-acetaldehyde, which were reduced by 44.13, 39.38 and 37.20%, respectively.

In addition to hydrogenation, the reduction in the concentration of identifiable compounds could be attributed to several other mechanisms. These potential pathways include the formation of undetectable compounds *via* polymerisation due
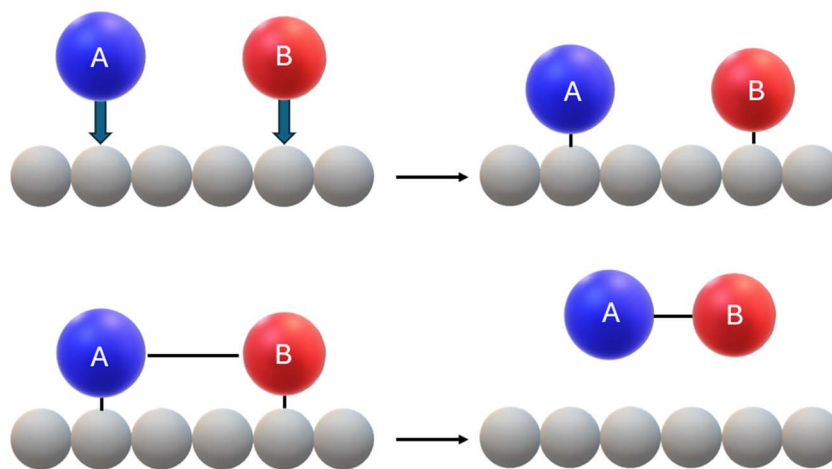

Fig. 3 Schematic of the Langmuir–Hinshelwood hydrogenation mechanism followed by organic compounds during EC. Reactants A and B adsorb onto the catalyst surface, react to form a product, which then desorbs from the surface. Where A is the organic compound, and B is hydrogen.

Table 1 Key composition of pine wood slow pyrolysis bio-oil aqueous phase before and after ECH

Compound	Before ECH (relative area)	After ECH (relative area)	Change in relative area	Change in concentration
4-Methyl-1,2-benzenediol	0.172	0.000	0.172	100.00%
3-Methyl-1,2-benzenediol	0.139	0.000	0.139	100.00%
p-Cresol	0.404	0.153	0.251	62.10%
2-Methyl-phenol	0.329	0.146	0.183	55.73%
3,5-Dimethyl-phenol	0.155	0.084	0.071	46.11%
5-Hydroxymethylfurfural	0.046	0.025	0.021	44.17%
Catechol	0.302	0.169	0.133	44.12%
2,5-Dimethyl-furan	0.348	0.237	0.111	31.73%
3-Methyl-2-cyclopenten-1-one	0.180	0.123	0.057	31.66%
Phenol	0.458	0.322	0.136	29.57%
Propanoic acid	0.064	0.058	0.006	8.23%
Butyrolactone	0.075	0.071	0.004	4.74%
Toluene	(1.00)	(1.00)	—	—

to their insolubility and higher boiling points, preferential adsorption of certain compounds onto the cathode and membrane, and conversion to products not readily identifiable by GC-MS. Although no coke formation was observed, adsorption onto the cathode did occur, necessitating cleaning after each experiment. Table 3 presents the major compounds before and after the control experiment (PW_{aq} added, constant temperature, no current), revealing the presence of non-electrochemical reactions.

Most compounds showed a reduction in concentration without the application of current, although they were, generally, lower than with current. For example, phenol is still converted without an applied current, dropping from 29.57% with current to 12.31% without. Similarly, 2-methyl-phenol, 3,5-dimethyl-phenol, catechol, and 3-methyl-2-cyclopenten-1-one, saw reductions in conversion rates from 55.73%, 46.11%, 44.12%, and 31.66% to 39.78%, 26.24%, 24.02%, and 4.32%, respectively.

Interestingly, both 4-methyl-1,2-benzenediol and 3-methyl-1,2-benzenediol are fully converted regardless of current input, indicating that non-electrochemical reactions drive their conversion. The formation of p-cresol likely results from these compounds' dehydration reaction, where an –OH group is lost. Notably, applying an overpotential reduced p-creosol concentration by 62.10%, indicating that hydrogenation of p-creosol significantly outweighs dehydration of 4-methyl-1,2-benzenediol and 3-methyl-1,2-benzenediol.

Conversely, butyrolactone showed a complete conversion, increasing from 4.74% with current (Table 1) to 100% without, likely forming butanoic acid and 4-hydroxy-butanoic acid, which increased significantly in concentration. This suggests that current suppresses the formation of these corrosive compounds, a favourable outcome for improving the bio-oil's properties. Similar results were found when the same experiment was conducted with WS_{aq}, including increased concentration of molecules containing carboxylic acid groups. These

Table 2 Key composition of wheat straw slow pyrolysis bio-oil aqueous phase before and after ECH

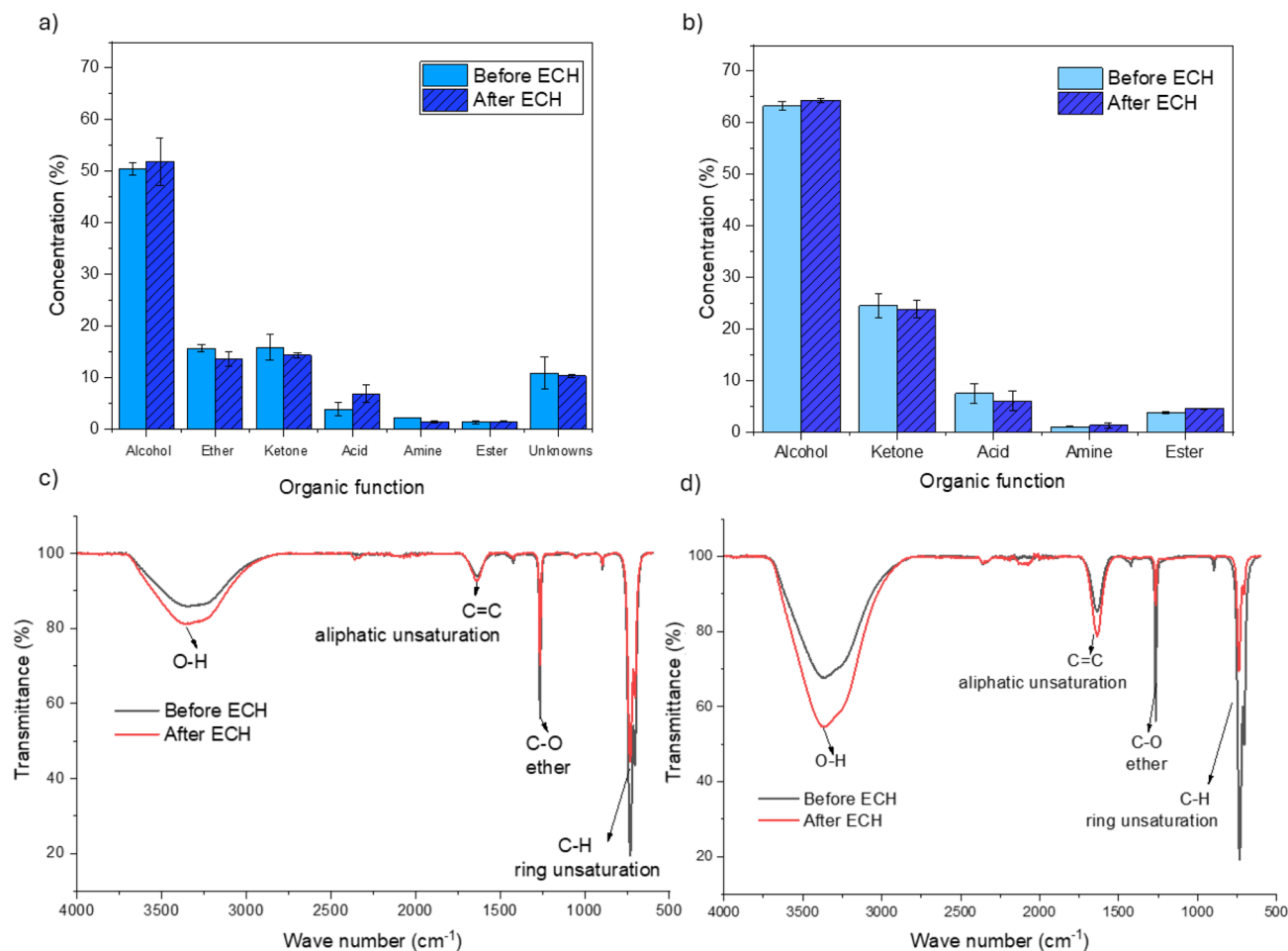| Compound	Before ECH (relative area)	After ECH (relative area)	Change in relative area	Change in concentration
Cyclopentanone	0.0251	0.0140	0.0111	44.13%
3,5-Dimethyl-phenol	0.0533	0.0323	0.0210	39.38%
2-Oxo-3-cyclopentene-1-acetaldehyde	0.1099	0.0690	0.0409	37.20%
p-Cresol	0.2216	0.1393	0.0823	37.13%
3-Ethyl-phenol	0.0489	0.0334	0.0155	31.69%
2-Methyl-phenol	0.1353	0.0970	0.0383	28.26%
4-Methyl-1,2-benzenediol	0.0765	0.0550	0.0215	28.04%
2-Methyl-2-cyclopenten-1-one	0.0346	0.0252	0.0094	26.98%
3-Methyl-1,2-benzenediol	0.0712	0.0524	0.0188	26.41%
3-Methyl-2-cyclopenten-1-one	0.0608	0.0449	0.0159	26.12%
Butyrolactone	0.0868	0.0649	0.0219	25.22%
Phenol	0.3368	0.2620	0.0748	22.20%
2-Methoxytetrahydrofuran	0.0514	0.0403	0.0111	21.52%
4-Ethyl-1,3-benzenediol	0.0360	0.0306	0.0054	15.07%
2-Cyclopenten-1-one	0.0454	0.0395	0.0059	13.03%
Catechol	0.1733	0.1521	0.0212	12.21%
Propanoic acid	0.0624	0.0593	0.0031	4.92%
Toluene	(1.00)	(1.00)	—	—

Fig. 4 Organic functions' relative concentration obtained by GC-MS (area%) in the slow pyrolysis of pinewood (a) and wheat straw (b) aqueous phases before and after ECH for 5 h. The FTIR spectrum is from the slow pyrolysis of pinewood (c) and wheat straw (d) aqueous phase before and after the ECH process, as well as the main identified peaks. Error bars indicate the standard error of triplicated experimental results.

findings highlight the need for applied current to drive selective hydrogenation effectively.

The observed decrease in the total concentration of reactants can be attributed to a combination of factors. While GC-MS analysis focuses on quantifiable changes in major compounds, the overall mass balance is influenced by (1) conversion to unidentifiable or undetectable products, (2) formation of higher molecular weight, less volatile compounds not detectable by GC-MS (potentially through polymerisation), and (3) adsorption onto the electrode. Our observations of no

Table 3 Key composition of pine wood slow pyrolysis bio-oil aqueous phase before and after the blank experiment, without current input

Compound	Before ECH (relative area)	After ECH (relative area)	Change in relative area	Change in concentration
4-Methyl-1,2-benzenediol	0.192	0.000	0.192	100.00%
3-Methyl-1,2-benzenediol	0.181	0.000	0.181	100.00%
Butyrolactone	0.131	0.000	0.131	100.00%
2-Methyl-phenol	0.546	0.328	0.218	39.78%
3,5-Dimethyl-phenol	0.249	0.183	0.066	26.24%
Catechol	0.457	0.347	0.110	24.02%
Phenol	0.719	0.631	0.088	12.31%
3-Methyl-2-cyclopenten-1-one	0.287	0.275	0.012	4.32%
p-Cresol	0.310	0.337	−0.027	−8.58%
Butanoic acid	0.123	0.167	−0.044	−35.08%
4-Hydroxy-butanoic acid	0.000	0.111	−0.111	−100.00%
Toluene	(1.00)	(1.00)	—	—

tar-like substance in the cathode chamber suggest a low tendency for significant polymerisation. Tests addressing evaporation showed no significant mass change. While adsorption of reactants or products onto the catalyst surface or electrochemical cell components is another potential loss pathway, GC-MS analysis of the extract from the cleaned cathode showed no discernible peaks, and the cathode's mass change post-reaction was less than 1%. Therefore, the formation of unidentifiable compounds *via* GC-MS and peak overlap is likely the primary contributor to the changes in mass balance. Further studies are needed to fully quantify the contribution of each of these factors to the overall mass balance.

3.2. ECH effect on organic functional groups

3.2.1. GC-MS analysis. GC-MS analysis (Fig. 4a) shows that the primary identifiable components in PW_{aq} are alcohols, ethers, and ketones. The increase in alcohol concentration (from 49.3% to 56.5%) after the ECH can be attributed to the reduction of ethers and ketones (from 16.3% and 18.3% to 12.2% and 13.8%, respectively), as hydrogenation of carbon–oxygen double bonds to C–OH is more easily achieved than full deoxygenation. Another notable finding is the 48% decrease in amine concentration, which is desirable since nitrogen removal is crucial in upgrading.

The effect of the hydrogenation process on carboxylic acids was examined in our previous study,[24] were we demonstrated that this group remains largely unaffected due to its stability and the specific hydrogenation mechanism. This same trend was observed in the ECH of PW_{aq}, where the process had little to no impact on the concentration of carboxylic acids. The identifiable compounds in WS_{aq} were also mainly alcohols, going from 63.2% to 64.3% after ECH (Fig. 4b). The concentration of ketones was reduced, while the ester concentration was slightly increased. The number of carboxylic acids, in contrast to PW_{aq}, also suffered a reduction, from 7.46 to 6.01%.

3.2.2. FTIR analysis. PW_{aq} FTIR analysis (Fig. 4c) reveals a significant increase in the peak at 3300 cm^{-1}, associated with the vibration of O–H groups found in alcohols and phenols following the ECH process. Additionally, there was a reduction in both the peak at 1240 cm^{-1}, linked to C–O in ether-containing compounds, and the peak at 700–750 cm^{-1}, indicating ring unsaturation vibrations. There is also a slight increase at 1640 cm^{-1}, possibly signifying the cleavage of phenyl groups into aliphatic compounds. Fig. 4d shows that WS_{aq} followed the same pattern, including a noticeable reduction in the concentration of unsaturated aromatic groups. This demonstrates that, although there wasn't a significant change in the organic group distribution, most of the double bonds in the aromatic rings were saturated. The reduction of ethers, increased alcohols, and aliphatic unsaturation were also higher in WS_{aq}.

The transformations observed through both GC-MS and FTIR are expected to improve fuel properties for the upgraded bio-oil. The reduction in oxygenated compounds, especially phenols and carboxylic acids, is beneficial for increasing the stability and calorific value of the bio-oil.[16,31] By converting these

compounds into more stable alcohols, the ECH process significantly enhances the overall quality of the bio-oil. However, direct measurement of these changes, such as by elemental analysis and calorimeter analysis, should be carried out in future work.

Moreover, the reduction in unsaturated aromatic rings improves the hydrogen-to-carbon ratio of the bio-oil. The increase in alcohol content, particularly cyclohexanol and other saturated alcohols, suggests that the fuel's energy density has been enhanced. While the aqueous phase itself is not suitable as a fuel due to its high water content, the changes detected by GC-MS and FTIR indicate the presence of valuable hydrogenated organic compounds. These compounds could be separated and utilised as fuel additives or feedstocks for further chemical processing towards fuel production. That is, the bio-oil's improved composition makes it more compatible with standard refining processes, increasing its potential for commercialisation.

3.3. Comparison with model compound behaviour

Phenol is more reactive to ECH than guaiacol,[24] probably due to guaiacol's more complex molecular structure. Both methoxy and phenolic groups on adjacent carbons in guaiacol increase bond energies, making it less reactive, whereas phenol's simpler structure facilitates hydrogenation. The presence of an electronegative substituent in the *ortho* position (guaiacol-like) can also hinder the approach of the catalyst and/or alter the electron density of the aromatic ring, making it less susceptible to hydrogenation compared to phenol-like compounds.

In this study, the compounds in WS_{aq} and PW_{aq} were classified as either "phenol-like" or "guaiacol-like" based on their structure. All these compounds contain a phenyl group (an alcohol attached to a benzene ring). Compounds with no additional substituents or a second substituent in the *meta* or *para* position were categorised as phenol-like. In contrast, compounds with an electronegative substituent (*e.g.*, alcohol or ether) in the *ortho* position were classified as guaiacol-like. Non-electronegative *ortho* substituents were also considered phenol-like. Although this is not an exhaustive list, most identified compounds could be categorised into these classifications. Fig. 5 shows some of the main compounds and their classification.

The higher concentration of phenol-like compounds in PW_{aq} (1.346 *vs.* internal standard) compared to WS_{aq} (0.831 *vs.* internal standard) indicates why it exhibited higher activity for ECH, achieving higher conversion rates on average (46.51 and 25.85%, respectively). These compounds, with less steric hindrance and simpler structures, were more readily hydrogenated than the "guaiacol-like" compounds.

The effect of the functional groups can be demonstrated by the conversion rates of *p*-creosol, 2-methyl-phenol, and catechol, where the methyl group goes from *para* to the *ortho* position, and the conversion (on average from the two feedstocks) goes from 49.61 to 42.00%, respectively. If the methyl group is substituted by an alcohol (catechol), a highly electronegative group, the conversion goes to 28.17%. Moving the
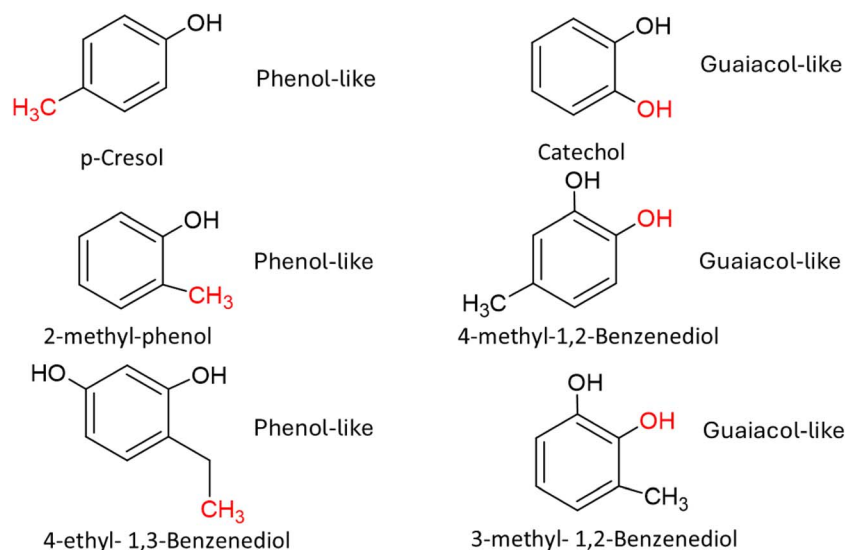
Fig. 5 Some of the main compounds in WS$_{aq}$ and PW$_{aq}$ and their classification in the system. The functional groups highlighted in red indicate the classification reasoning.

methyl group from *para* (4-methyl-1,2-benzenediol) to *meta* (3-methyl-1,2-benzenediol) also reduced the conversion rate, from 64.02 to 63.21%.

4. Conclusion

This study demonstrates the effectiveness of electrochemical hydrogenation in upgrading the aqueous phase from bio-oil derived from the slow pyrolysis of wheat straw and pinewood. The process successfully reduces oxygenated compounds, particularly phenols, while increasing the concentration of alcohols, thereby improving the stability and energy density of the bio-oil. FTIR and GC-MS analyses confirmed these transformations, showing that ECH preferentially saturates aromatic rings and increases hydrogen content without needing high-pressure hydrogen gas.

However, certain limitations were observed. The incomplete conversion of compounds like catechol and the formation of minor side products such as cyclohexanone indicate that further optimisation of reaction conditions is necessary to achieve more efficient and complete conversions. Additionally, the resistance of carboxylic acids to hydrogenation poses a challenge for fully upgrading the bio-oil to high-quality fuels. Addressing these issues will be crucial in refining the process for more consistent and predictable outcomes.

Despite these challenges, the ECH process shows strong potential for scale-up. The lab-scale results suggest that industrial applications are feasible, particularly given the process's lower energy requirements compared to traditional hydrodeoxygenation methods. Future work will focus on developing pilot-scale systems that continuously process larger volumes of bio-oil while ensuring catalyst regeneration and maintaining process efficiency. By addressing the current challenges and demonstrating scalability, ECH could become a viable method for producing renewable fuels from biomass, supporting the global shift towards cleaner energy sources.

Author contributions

C. Catizane conducted the experimental work and analysis/imaging and was the primary author of the paper. J. Sumner and Y. Jiang supervised the research, revised the manuscript and contributed to the technical content of the paper. S. Banks revised the manuscript and contributed to the technical content of the paper.

Conflicts of interest

There are no conflicts to declare.

Data availability

The source data supporting this study's findings are available from the Figshare repository (**https://doi.org/10.6084/m9.figshare.28435610.v1**).

Acknowledgements

References

1 S. H. Chang, Plastic waste as pyrolysis feedstock for plastic oil production: A review, *Sci. Total Environ.*, 2023, **877**, 162719.

2 S. Singh, J. P. Chakraborty and M. K. Mondal, Pyrolysis of torrefied biomass: Optimization of process parameters using response surface methodology, characterization, and comparison of properties of pyrolysis oil from raw biomass, *J. Cleaner Prod.*, 2020, **272**, 122517.

3 J. He, V. Strezov, T. Kan, H. Weldekidan and R. Kumar, Slow pyrolysis of metal(loid)-rich biomass from phytoextraction: characterisation of biomass, biochar and bio-oil, *Energy Procedia*, 2019, **160**, 178–185.

4 Z. Luo, *et al.*, Research on biomass fast pyrolysis for liquid fuel, *Biomass Bioenergy*, 2004, **26**, 455–462.

5 F. Stankovikj, A. G. Mcdonald, G. L. Helms, M. V. Olarte and M. Garcia-Perez, Characterization of the Water-Soluble Fraction of Woody Biomass Pyrolysis Oils, *Energy Fuels*, 2017, **31**(2), 1650–1664.

6 K. Sipilä, E. Kuoppala, L. Fagernäs and A. Oasmaa, Characterization of biomass-based flash pyrolysis oils, *Biomass Bioenergy*, 1998, **14**, 103–113.

7 Q. Zhang, J. Chang, T. Wang and Y. Xu, Review of biomass pyrolysis oil properties and upgrading research, *Energy Convers. Manage.*, 2007, **48**, 87–92.

8 R. Kumar and V. Strezov, Thermochemical production of bio-oil: A review of downstream processing technologies for bio-oil upgrading, production of hydrogen and high value-added products, *Renewable Sustainable Energy Rev.*, 2021, **135**, 110152.

9 S. Hansen, A. Mirkouei and L. A. Diaz, A comprehensive state-of-technology review for upgrading bio-oil to renewable or blended hydrocarbon fuels, *Renewable Sustainable Energy Rev.*, 2020, **118**, 109548.

10 R. E. Guedes, A. S. Luna and A. R. Torres, Operating parameters for bio-oil production in biomass pyrolysis: A review, *J. Anal. Appl. Pyrolysis*, 2018, **129**, 134–149.

11 Z. Li, M. Garedew, C. Lam, J. Jackson, D. Miller and C. Saffron, Mild electrocatalytic hydrogenation and hydrodeoxygenation of bio-oil derived phenolic compounds using ruthenium supported on activated carbon cloth, *Green Chem.*, 2012, **14**, 2540–2549.

12 G. Chen, *et al.*, Upgrading of Bio-Oil Model Compounds and Bio-Crude into Biofuel by Electrocatalysis: A Review, *ChemSusChem*, 2021, **14**, 1037–1052.

13 I. Graça, J. M. Lopes, H. S. Cerqueira and M. F. Ribeiro, Bio-oils Upgrading for Second Generation Biofuels, *Ind. Eng. Chem. Res.*, 2012, **52**, 275–287.

14 J. D. Adjaye and N. N. Bakhshi, Catalytic conversion of a biomass-derived oil to fuels and chemicals I: Model compound studies and reaction pathways, *Biomass Bioenergy*, 1995, **8**, 131–149.

15 P. M. Mortensen, J. D. Grunwaldt, P. A. Jensen, K. G. Knudsen and A. D. Jensen, A review of catalytic upgrading of bio-oil to engine fuels, *Appl. Catal., A*, 2011, **407**, 1–19.

16 B. Zhang, J. Zhang and Z. Zhong, Low-Energy Mild Electrocatalytic Hydrogenation of Bio-oil Using Ruthenium Anchored in Ordered Mesoporous Carbon, *ACS Appl. Energy Mater.*, 2018, **1**, 6758–6763.

17 Y. Zhou, *et al.*, Electrocatalytic Upgrading of Lignin-Derived Bio-Oil Based on Surface-Engineered PtNiB Nanostructure, *Adv. Funct. Mater.*, 2019, **29**, 1807651.

18 A. Gutierrez, R. K. Kaila, M. L. Honkela, R. Slioor and A. O. I. Krause, Hydrodeoxygenation of guaiacol on noble metal catalysts, *Catal. Today*, 2009, **147**, 239–246.

19 Y. H. E. Sheu, R. G. Anthony and E. J. Soltes, Kinetic studies of upgrading pine pyrolytic oil by hydrotreatment, *Fuel Process. Technol.*, 1988, **19**, 31–50.

20 W. Baldauf, U. Balfanz and M. Rupp, Upgrading of flash pyrolysis oil and utilization in refineries, *Biomass Bioenergy*, 1994, **7**, 237–244.

21 J. Wildschut, F. H. Mahfud, R. H. Venderbosch and H. J. Heeres, Hydrotreatment of Fast Pyrolysis Oil Using Heterogeneous Noble-Metal Catalysts, *Ind. Eng. Chem. Res.*, 2009, **48**(23), 10324–10334.

22 P. T. Williams and P. A. Horne, Characterisation of oils from the fluidised bed pyrolysis of biomass with zeolite catalyst upgrading, *Biomass Bioenergy*, 1994, **7**, 223–236.

23 A. R. K. Gollakota, M. Reddy, M. D. Subramanyam and N. Kishore, A review on the upgradation techniques of pyrolysis oil, *Renewable Sustainable Energy Rev.*, 2016, **58**, 1543–1568.

24 C. Catizane, Y. Jiang and J. Sumner, Mechanisms of electrochemical hydrogenation of aromatic compound mixtures over a bimetallic PtRu catalyst, *Commun. Chem.*, 2025, **8**, 56.

25 C. Catizane, Y. Jiang and J. Sumner, Hydrogen bond enhanced electrochemical hydrogenation of benzoic acid over a bimetallic catalyst, *Sustainable Energy Fuels*, 2025, **9**, 3014–3022.

26 Y. Du, X. Chen and C. Liang, Selective electrocatalytic hydrogenation of phenols over ternary Pt3RuSn alloy, *Mol. Catal.*, 2023, **535**, 112831.

27 S. Salakhum, T. Yutthalekha, S. Shetsiri, T. Witoon and C. Wattanakit, Bifunctional and Bimetallic Pt–Ru/HZSM-5 Nanoparticles for the Mild Hydrodeoxygenation of Lignin-Derived 4-Propylphenol, *ACS Appl. Nano Mater.*, 2019, **2**, 1053–1062.

28 J. Peng, *et al.*, Effect of Boiling Pretreatment on Physicochemical and Transport Properties of Perfluorosulfonic Acid Membrane, *ACS Appl. Polym. Mater.*, 2023, **5**, 9940–9951.

29 Y. Du, X. Chen, W. Shen, H. Liu, M. Fang, J. Liu and C. Liang, Electrocatalysis as an efficient alternative to thermal catalysis over PtRu bimetallic catalysts for hydrogenation of benzoic acid derivatives, *Green Chem.*, 2023, **25**, 5489–5500.

30 C. Liu, F. Chen, B.-H. Zhao, Y. Wu and B. Zhang, Electrochemical hydrogenation and oxidation of organic species involving water, *Nat. Rev. Chem.*, 2024, **8**, 277–293.

31 Z. Li, *et al.*, A mild approach for bio-oil stabilization and upgrading: electrocatalytic hydrogenation using ruthenium supported on activated carbon cloth, *Green Chem.*, 2014, **16**, 844–852.

32 R. Qu, K. Junge and M. Beller, Hydrogenation of Carboxylic Acids, Esters, and Related Compounds over Heterogeneous Catalysts: A Step toward Sustainable and Carbon-Neutral Processes, *Chem. Rev.*, 2023, **123**, 1103–1165.

33 S. J. Blanksby and G. B. Ellison, Bond Dissociation Energies of Organic Molecules, *Acc. Chem. Res.*, 2003, **36**, 255–263.